Correspondence

Potential of Acoustic Imaging in the Detection of Nanometer Gaps

Hironori Tohmyoh, Masumi Saka, and Hayato Hirayama

***Abstract*—The potential of the water-immersion and dry-contact acoustic imaging techniques for detecting nanometer gaps embedded in silicon is studied. The sensitivity for detecting gaps of over 10 nm in height is governed only by the lateral resolution of the imaging and is independent of the height of the gap.**

I. Introduction

Acoustic microscopy/imaging is a standard tool for the nondestructive detection and evaluation of defects in samples [1], [2]. The recent trend toward micro- and nanotechnologies has brought added complexity to the structures of typical samples, e.g., multilayered structures for microelectronic packages [3], and these require higher-quality, cross-sectional images, including information about micro- and nanoscale defects. Hsu and Dayal [4] reported on interactions between acoustic waves and thin gaps by conducting Newton's ring experiments. However, the detectable size of defects embedded in samples is yet to be clarified. Acoustic imaging usually has to be performed by immersing the samples in water, which limits the types of samples that can be analyzed. An alternate dry-contact acoustic technique recently was reported that achieves the transduction of high-frequency ultrasound under a dry environment via a solid layer [5]. Furthermore, it has been discovered that the signal intensity of ultrasound transmitted into silicon (which is the most important material in micro/nanoelectro mechanical systems) via a polymer layer exceeds that achieved in the case of water immersion due to an ultrasonic resonance that occurs between the water, the layer, and the silicon [6].

In this paper, silicon bonding samples with precise nanometer gaps are fabricated by a fast-atom-beam etching and direct bonding technique; and the sensitivity for acoustic detection of the embedded gaps is studied using both the conventional water-immersion technique and a dry-contact technique. For the dry-contact technique, a polymer acoustic matching layer is inserted between the water and the silicon. The potential of the dry-contact acoustic imaging technique for detecting nanometer gaps embedded in silicon (i.e., the signal intensity and the spatial resolution) is compared with that of the water-immersion technique.

Manuscript received October 8, 2005; accepted July 7, 2006. This work was partly supported by the Ministry of Education, Culture, Sports, Science and Technology, Japan, under a Grant-in-Aid for Young Scientists (B) 17760072 and by the Ono Acoustics Research Fund. A part of this work was performed at the Venture Business Laboratory at Tohoku University.

The authors are with Tohoku University, Department of Nanomechanics, Sendai 980-8579, Japan (e-mail: tohmyoh@ism.mech.tohoku.ac.jp).

Digital Object Identifier 10.1109/TUFFC.2006.196

II. Principle of Dry Ultrasonic Transmission

The dry-contact acoustic technique transmits ultrasound via a solid layer inserted between the water and the sample. A pressure of about 0.1 MPa is applied to the contacting interface between the layer and the sample by evacuating the air from between them [5]. The surface roughness of the sample and the elastic deformation of both the solid layer and the sample, accompanied by the ultrasonic transmission, usually result in air-gaps forming at the contacting interface [7], [8]. Thus, the application of pressure to the layer/sample interface is effective for improving the acoustic coupling between the different components [5]. The efficiency of ultrasonic transmission via a solid layer compared with the water-immersion case, γ, can be expressed as:

$$\gamma = \phi_1/\phi_2 = \theta\xi\psi, \tag{1}$$

where ϕ is the amplitude spectrum of the echo from the objective interface, and the subscripts 1 and 2 imply dry-contact and water-immersion cases, respectively. The terms ξ and ψ represent the signal losses related to the ultrasonic attenuation in the layer and the acoustic coupling at the layer/sample interface; and these become unity under the no-loss condition. The term θ is related to the acoustic impedance matching between the water and the sample. If we consider plane waves of frequency ν, then this takes its maximum value at the layer thickness given by:

$$d = (c_L/4\nu_r), \tag{2}$$

where c_L is the longitudinal wave velocity in the layer, ν_r is the resonance frequency, and d is well-known as the condition for a quarter-wave matching layer [9], [10]. The maximum value of θ at ν_r is given by:

$$\theta_r = \left[Z_L^2\left(Z_W + Z_S\right)^2\right] / \left[\left(Z_W Z_S + Z_L^2\right)^2\right], \tag{3}$$

where Z_W ($= 1.51$ MNm^{-3}s), Z_L and Z_S are the acoustic impedances of water, the layer, and the sample, respectively. The value of θ is greater than unity for the effective frequency range $0 < \nu/\nu_r < 2$ [11].

III. Experiments

Three chips measuring $20 \times 20 \times 0.5$ mm were cut-out from silicon [100] wafers. Grooves were patterned on

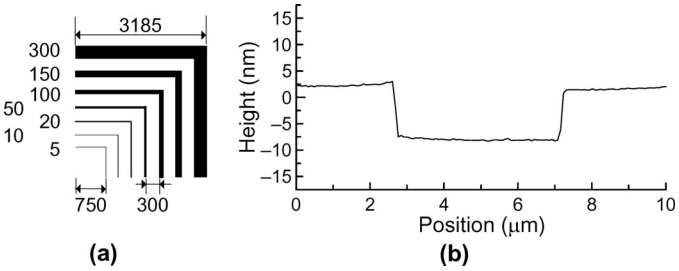

Fig. 1. Silicon bonding sample. (a) Patterned nanometer gaps (units are in μm). (b) An example of the height profile around a 5-μm wide gap obtained by AFM.

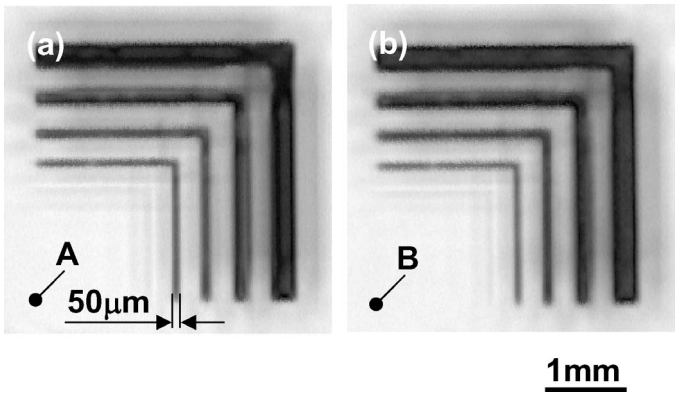

Fig. 2. Acoustic images of a silicon bonding sample recorded under (a) water immersion, and (b) a PVDC-contact.

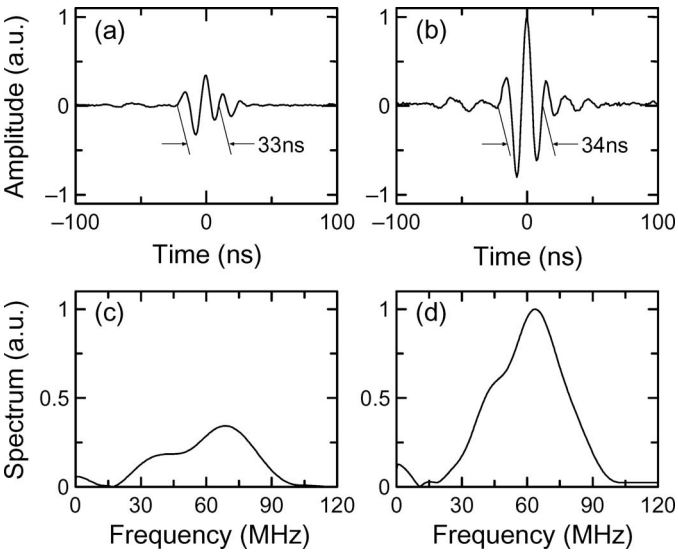

Fig. 3. Waveforms obtained under (a) water immersion, and (b) a PVDC-contact. The amplitude spectra of (a) and (b) are shown in (c) and (d), respectively.

two of the silicon chips by using photolithography and a fast-atom-beam etching technique, as shown in Fig. 1(a). Similar patterns were previously used for determining the lateral resolution of the acoustic imaging [12]. All of the chips (including the nonpatterned chip) then were subjected to a standard RCA clean. Because the height of the gaps that were introduced would be altered by any further oxidation, the silicon dioxide layers were completely removed from all of the chips at this stage by using hydrofluoric acid. One of the two patterned silicon chips was used to measure the height of the gaps. Fig. 1(b) shows an example of a height profile around a 5 μm-wide gap as obtained by atomic force microscopy (AFM), and the heights of the introduced gaps were confirmed to be 9.7 ± 0.4 nm. The other patterned chip and the nonpatterned chip were bonded using an EV520 wafer bonder (EV Group, Schardinger, Austria) immediately after a standard RCA clean, and a silicon bonding sample of 1 mm in thickness with precise nanometer gaps ($Z_S = 20.74$ MNm^{-3}s) was obtained. Another silicon bonding sample with 106 ± 2 nm height gaps was prepared by the same procedure. Pure water at 295 K was used as the coupling liquid. A broadband ultrasonic transducer that had a nominal frequency of 100 MHz, a 6.35 mm piezoelectric element, and a focal length of 12.7 mm was used to record the acoustic images at the back walls of samples that faced air in both cases with and without the intermediate layer. We used poly(vinylidene chloride) (PVDC), as the intermediate layer for the dry-contact technique in this work because it has a larger value of Z_L (= 3.23 MNm^{-3}s) than many other polymer materials. The value of c_L was 1964 m/s, and d was set at 9 μm by taking into account the frequency characteristics of used ultrasonic transducer. The PVDC layer was expected to behave as an acoustic matching layer between 0 and 109.1 MHz ($\theta_r = 3.0$, $\nu_r = 54.6$ MHz). The details of the dry-contact unit used in the experiments are described elsewhere [5].

IV. Results and Discussion

Acoustic images of silicon bonding sample with 10-nm gaps recorded under water immersion and PVDC-contact are shown in Figs. 2(a) and (b), respectively. Both the water-immersion and the PVDC-contact images clearly depict gaps that are wider than 50 μm. In Fig. 2, no conspicuous differences between the water-immersion and the PVDC-contact images can be observed. Figs. 3(a) and (b) show the waveforms obtained under water immersion and PVDC-contact at points A and B in Fig. 2, respectively. The sum of the periods for the PVDC-contact, which was determined between the first and the second waves, was 34 ns; this was almost the same as that for water immersion (33 ns). This indicated that the time resolution of the PVDC-contact imaging technique was equivalent to that of the usual water-immersion technique. Figs. 3(c) and (d) show the amplitude spectra of the waveforms shown in Figs. 3(a) and (b), respectively. Fig. 3(d) clearly shows that the transmission of the broadband ultrasound was realized more effectively via the PVDC layer than by the usual water-immersion method [Fig. 3(c)] in the frequency range between 20 and 100 MHz. The peak frequency using the PVDC-contact was 63.5 MHz, which was close to that obtained using water immersion (68.8 MHz). The maximum value of γ was 3.4 at 55.7 MHz, and these values

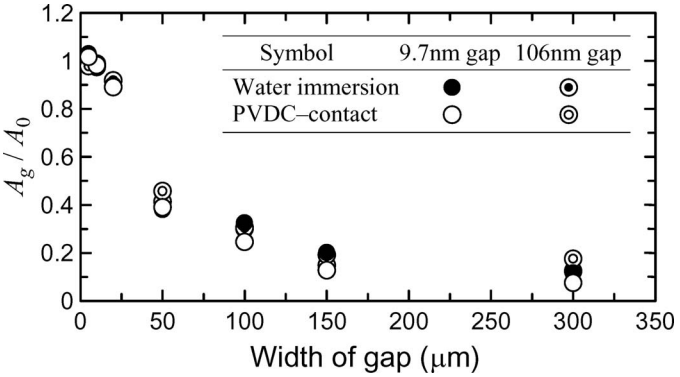

Fig. 4. Relationships between A_g/A_0 and the gap width.

were close to θ_r (= 3.0) at ν_r (= 54.6 MHz). This indicated that the values of ξ and ψ were close to unity, and that the PVDC layer behaved as we expected as a matching layer. The lateral resolution is defined as the separable distance between two sound sources in an objective plane, and it can be estimated from the amplitude spectrum [13]. The lateral resolution of the PVDC-contact was estimated as 46 μm; this value was almost the same as that obtained by water immersion (45 μm). The acoustic images shown in Fig. 2 supported the validity of this estimation, and the clearness of the gaps in Fig. 2 was in good agreement with the estimated lateral resolution.

Let us now consider the sensitivity for detecting gaps by using the relative intensity of the back-wall echo (= A_g/A_0) as a measure in which A_0 is the amplitude of the echo from the back of the sample obtained at a position without a gap, and A_g is that obtained at the center of a gap. Lower values of A_g/A_0 indicate higher sensitivity to embedded gaps. Fig. 4 shows the relationships between A_g/A_0 and the width of the gap. For the gap widths we examined, there was no difference in the values of A_g/A_0 between the water-immersion and the PVDC-contact imaging techniques, and no difference was also observed in the values of A_g/A_0 for gaps between 10 nm and 106 nm in height. The experimental evidence suggests that the sensitivity for detecting nanometer gaps using PVDC-contact imaging was the same as that for water-immersion imaging. In the acoustic imaging techniques we made, the gap height has no influence on the sensitivity for detecting embedded gaps up to 300 μm wide when the height of the gaps is over 10 nm. The values of A_g/A_0 for all combinations of imaging and gap heights took constant values for gaps over 150 μm wide; and these increased with decreasing gap width. The gaps that were narrower than 50 μm were difficult to identify when using both the water-immersion and the PVDC-contact imaging techniques. The increases in the values of A_g/A_0 were closely related with the acoustic focusing in the samples; therefore, the detectable size of gaps embedded in silicon was governed only by the lateral resolution of the imaging method we used. In this study, the objective interfaces were located at a depth of 1 mm from the sample surface. For the inspection of very small defects that are deeper in a silicon structure, the dry-contact acoustic technique with a suitable matching layer has an advantage over the water-immersion technique from the point of view of the signal intensity that can be obtained.

V. Conclusions

The relative benefits of the water-immersion and the dry-contact acoustic imaging techniques for the detection of nanometer gaps embedded in silicon bonding samples were compared. The signal intensity obtained by dry-contact technique via a poly(vinylidene chloride) acoustic matching layer exceeded that of the water-immersion technique. The spatial resolution for dry-contact imaging (i.e., the time resolution and the lateral resolution) was verified to be the same as that of the water-immersion imaging. Both the water-immersion and dry-contact imaging techniques were able to detect very-low-scale, embedded gaps that were over 10 nm in height, and the sensitivity for detecting small gaps was governed only by the lateral resolution of the imaging method used. We concluded that dry-contact acoustic imaging is suitable for the detection of nanometer gaps in samples without having to immerse the sample in water.

References

[1] Z. Yu and S. Boseck, "Scanning acoustic microscopy and its applications to material characterization," *Rev. Mod. Phys.*, vol. 67, no. 4, pp. 863–891, 1995.

[2] R. S. Gilmore, "Industrial ultrasonic imaging and microscopy," *J. Phys. D: Appl. Phys.*, vol. 29, no. 6, pp. 1389–1417, 1996.

[3] G.-M. Zhang, D. M. Harvey, and D. R. Braden, "High-resolution AMI technique for evaluation of microelectronic packages," *Electron. Lett.*, vol. 40, no. 6, pp. 399–400, 2004.

[4] D. K. Hsu and V. Dayal, "Ultrasonic Newton's rings," *Appl. Phys. Lett.*, vol. 60, no. 10, pp. 1169–1171, 1992.

[5] H. Tohmyoh and M. Saka, "Dry-contact technique for high-resolution ultrasonic imaging," *IEEE Trans. Ultrason., Ferroelect., Freq. Contr.*, vol. 50, no. 6, pp. 661–667, 2003.

[6] H. Tohmyoh and M. Saka, "Design and performance of a thin, solid layer for high-resolution, dry-contact acoustic imaging," *IEEE Trans. Ultrason., Ferroelect., Freq. Contr.*, vol. 51, no. 4, pp. 432–438, 2004.

[7] B. Drinkwater, R. Dwyer-Joyce, and P. Cawley, "A study of the transmission of ultrasound across solid-rubber interfaces," *J. Acoust. Soc. Amer.*, vol. 101, no. 2, pp. 970–981, 1997.

[8] J.-Y. Kim, A. Baltazar, and S. I. Rokhlin, "Ultrasonic assessment of rough surface contact between solids from elastoplastic loading-unloading hysteresis cycle," *J. Mech. Phys. Solids*, vol. 52, no. 8, pp. 1911–1934, 2004.

[9] L. M. Brekhovskikh, in *Waves in Layered Media*. New York: Academic, 1960, pp. 44–61.

[10] C. S. Desilets, J. D. Fraser, and G. S. Kino, "The design of efficient broad-band piezoelectric transducers," *IEEE Trans. Sonics Ultrason.*, vol. SU-25, no. 3, pp. 115–125, 1978.

[11] H. Tohmyoh, "Polymer acoustic matching layer for broadband ultrasonic applications," *J. Acoust. Soc. Amer.*, vol. 120, no. 1, pp. 31–34, 2006.

[12] Y. Ogura, "High-sensitivity detection of voids at direct wafer-bonding interface by ultrasonic imaging method," *OYO BUTURI*, vol. 66, no. 5, pp. 467–471, 1997. (in Japanese)

[13] S. Canumalla, "Resolution of broadband transducers in acoustic microscopy of encapsulated ICs: Transducer selection," *IEEE Trans. Comp. Packag. Technol.*, vol. 22, no. 4, pp. 582–592, 1999.